eJSE International
Electronic Journal of Structural Engineering 14 - 2014

Optimization of Interference Effects on High-Rise Buildings for Different Wind Angle Using CFD Simulation

A.K. Bairagi* & S.K. Dalui
Department of Civil Engineering, Indian Institute of Engineering Science and Technology, Shibpur, Howrah, India, 711 103.

*bairagiak@gmail.com

ABSTRACT: A numerical study by CFD (Computational Fluid Dynamics) simulation to obtain optimum spacing in between interfering and principal building where the interference effects are nullified and the behavior of principal building will be the same as the isolated building. The analytical result of rectangular plan shape prismatic bluff bodies are investigated in a series of Fluid Flow (CFX) analysis to study the optimum spacing in between interfering and principal building at 0° and 90° wind angle. This study highlights the Interference Factor (IF) of principal building which is similar to the an isolated building due to increasing spacing in between interfering and principal building. The plans of both the buildings are rectangular in shape and similar dimensions and principle axis. This study also highlights the IF, also found by the graphical representation of different spacing between interfering building and principal building.

Keywords: Computational Fluid Dynamics, Interfering Building, Interference Factor, Optimum spacing

1 INTRODUCTION

Urban areas with high-rise buildings of high density were used to minimize the quantity of land. The wind force acting on those principal buildings are quite different than the wind force acting on the isolated buildings. The present study investigates the optimum spacing between interfering and principal building where the turbulence developed by the interfering building doesn't affect the principal building. The interfering building and principal building of symmetrical rigid bluff bodies have rectangular cross-sections. In this study Computational Fluid Dynamics (CFD) is used to compute wind flow around a row of two buildings at wind angle 0^0 and 90^0. The two buildings are in same size and parallel to each other. The Depth (D) 250 mm, Width (W) 100 mm, Height (H) 500 mm and initial Spacing (S) 200 mm adopted for the building models. Xie and Gu (2004) give the general guideline to the mean interference effects between two and among three tall buildings are of the same height, the shielding effect increases and therefore the interference factor (IF) decreases with the increase of the breadth of the interfering buildings. However, due to the channeling effects, two adjacent interfering buildings can significantly enhance the mean wind load on the principal building. Using by CFD and wind tunnel test was carried out by the Blocken. et al. in (2007) who studied the wind tunnel test as well as CFD test for determining the venture-effects on the increase of wind speed in passages at the pedestrian level and that the flow rate through the passage is almost 8% higher than the free-field flow rate. Mendis et al. (2007) provides an outline of advanced levels of wind design and illustrates the exceptional benefits which offers over simplified approaches and also highlight interference from other structures, wind directionality, and cross wind response, which are all important factors in wind design of tall buildings. Braun and Awruch (2009) tried to give general guide line of the aerodynamic and aero-elastic analyses on the CAARC (Commonwealth Advisory Aeronautical Council) standard tall building model for measurements of pressure and aerodynamic coefficients were performed over the building surface and the agreement with other experimental and numerical predictions was satisfactory when smooth flows or low turbulence conditions were considered by the reference studies. Agerneh et al. (2009) present the CARRC model has been used extensively to study wind loading on tall buildings by using wind tunnel studies and is usually adopted for calibration of experimental techniques by CFD. Numerically obtained pressure coefficients on the surface of CAARC building under different configurations of adjacent building are compared with wind tunnel data collected from the laboratory. Hui et al. (2013)

investigates the interference effects between two rectangular section high-rise buildings by wind tunnel experiments were carried out under 72 wind incidence angles for various configurations. The interference factors for the largest positive peak pressure were in the range of 0.9-1.1. It exceeded 1.2 for only one configuration of the perpendicular arrangement. However, the interfering building has a very strong effect on the smallest negative peak pressure. This paper highlights the optimum spacing in between interfering and principal building where the interference doesn't affect the principal building. For 0° and 90° wind angle, Interference Factor (IF) are presented in this paper which can be calculated by plotting on graphical representation of required spacing between two buildings lies in same axis and same dimensions. IF can be multiplied for designing the high rise buildings for wind action.

2 NUMERICAL STUDY

In Computational Fluid Dynamics (CFD) the *k-epsilon* model is broadly used. The *k-ε* models use the gradient diffusion hypothesis to relate the Reynolds stresses to the mean velocity gradients and the turbulent viscosity. Turbulence intensity was considered as 10%. The turbulent viscosity is modelled as the product of a turbulent velocity and turbulent length scale. *k* is the turbulence kinetic energy and is defined as the variance of the fluctuations in velocity. It has dimensions of (L^2T^2); for example, m^2/s^2. *ε* is the turbulence eddy dissipation and has dimensions of per unit time (L^2T^3); for example, m^2/s^3.

The *k-ε* model introduces two new variables into the system of equations. The continuity equation is then:

$$\frac{\partial \rho}{\partial t} + \frac{\partial}{\partial x_j}\left(\rho U_j\right) = 0 \tag{1}$$

And the momentum equation will be

$$\frac{\partial \rho U_i}{\partial t} + \frac{\partial}{\partial x_j}\left(\rho U_i U_j\right) = -\frac{\partial p'}{\partial x_i} + \frac{\partial}{\partial x_j}\left[\mu_{eff}\left(\frac{\partial U_i}{\partial x_j} + \frac{\partial U_i}{\partial x_I}\right)\right] + S_M \tag{2}$$

where *U*= vector of velocity; *i,j*= direction of fluid element; *ρ*= density of air = 1.224 kg/m^3; μ_{eff} = effective viscosity accounting for turbulence; S_M = sum of body forces; *p´*= modified pressure as defined by:

$$p + \frac{2}{3}\rho k + \frac{2}{3}\mu_{eff}\frac{\partial U_k}{\partial k} \tag{3}$$

The last term in equation (3) i.e. $(2/3\,\mu\_eff\ (\partial U\_k)/\partial k)$ involves the divergence of velocity. It is neglected in CFX. Therefore this assumption is strictly correct only for incompressible fluids. The *k-ε* model is based on the eddy viscosity concept, so that:

$$\mu_{eff} = \mu + \mu_t \tag{4}$$

where μ_{eff}= effective viscosity, μ= molecular (dynamic) viscosity; μ_t= turbulence viscosity.
The *k-ε* model assumes that the turbulence viscosity is linked to the turbulence kinetic energy and dissipation via the relation:

$$\mu_t = C_\mu \rho \frac{k^2}{\varepsilon} \tag{5}$$

The values of *k* and *ε* come directly from the differential transport equations for the turbulence kinetic energy and turbulence dissipation rate:

$$\frac{\partial(\rho k)}{\partial t} + \frac{\partial}{\partial x_j}\left(\rho k U_j\right) \tag{6}$$

$$= \frac{\partial}{\partial x_j}\left[\left(\mu + \frac{\mu_t}{\sigma_k}\right)\frac{\partial k}{\partial x_j}\right] + P_k + P_b - \rho\varepsilon - Y_M + S_k$$

$$\frac{\partial(\rho\varepsilon)}{\partial t} + \frac{\partial}{\partial x_j}\left(\rho\varepsilon U_j\right)$$

$$= \frac{\partial}{\partial x_j}\left[\left(\mu + \frac{\mu_t}{\sigma_\varepsilon}\right)\frac{\partial \varepsilon}{\partial x_j}\right] + \rho C_1 S_\varepsilon - \rho C_2 \frac{\varepsilon^2}{k+\sqrt{v\varepsilon}} + C_{1\varepsilon}\frac{\varepsilon}{k}C_{3\varepsilon}P_b + S_\varepsilon \tag{7}$$

where

$$C_1 = max\left[0.43, \frac{\eta}{\eta+5}\right];\ \eta = S\frac{k}{\varepsilon};\ S = \sqrt{2S_{ij}S_{ij}}$$

Here P_k = the generation of turbulence kinetic energy due to the mean velocity gradients; P_b = the generation of turbulence kinetic energy due to buoyancy; Y_M = the contribution of the fluctuating dilatation in compressible turbulence to the overall dissipation rate. *S*= modulus of the mean rate-of-strain tensor, *Cμ, C1ε, C2, σk,* and σ_ε are constants refer Table 1.

Table 1. Values of model constants.

Symbol	Description	Value
C_μ	*k-ε* turbulence model constant	0.09
$C_{1\varepsilon}$	*k-ε* turbulence model constant	1.44
C_2	*k-ε* turbulence model constant	1.92
σ_k	Turbulence model constant for the *k* equation	1.0
σ_ε	*k-ε* turbulence model constant	1.2

3 EVALUATION OF WIND LOAD AS PER IS 875: (Part-3)-1987

The basic wind speed *(V_b)* for any site shall be obtained from Figure 1 of IS: 875 (Part 3)-1987 and shall be modified to include the following effects to get design wind velocity at any height *(Vz)* for the chosen structure:

i. Risk level
ii. Terrain roughness, height and size of structure and
iii. Local topography.

It can be mathematically expressed as follows:

$$V_z = V_b \times k_1 \times k_2 \times k_3 \quad (8)$$

where V_z = design wind speed at any height z in m/s; k_1 = probability factor or risk coefficient (k_1 ranging from 0.67 to 1.08); k_2 = terrain, height and structure size factor (k_2 ranging from 0.67 to 1.40); and k_3 = topography factor (k_3 ranging from 1.00 to 1.36)

The design wind pressure at any height above mean ground level shall be obtained by the following relationship between wind pressure and wind velocity:

$$P_d = 0.6 \times V_z^{\,2} \quad (9)$$

where P_d = design wind pressure in N/m^2 at height z; and V_z = design wind velocity in m/s at height z.

While calculating the wind load on individual structural elements such as roofs and walls, and individual cladding units and their fittings, it is essential to take account of the pressure difference between opposite face, of such elements or units. For clad structures, it is therefore necessary to know the internal pressure as well as the external pressure. Then the wind load, F acting in a direction normal to the individual structural element or cladding unit is:

$$F = \left(C_{pe} - C_{pi}\right) \times A \times P_d \quad (10)$$

where C_{pe} = external pressure coefficient; C_{pi} = internal pressure coefficient; A = surface area of structural or cladding unit; and P_d = design wind pressure.

The external pressure coefficient (C_{pe}) can be obtained from Table: 4 of IS: 875 (Part 3)-1987. The value of external pressure coefficient are consider after satisfying some conditions. In this study the condition $\frac{3}{2} < \frac{h}{w} < 6$, $\frac{3}{2} < \frac{l}{w} < 4$ are satisfying with Table: 4 of IS: 875 (Part 3)-1987. Where h is the height of structure above mean ground level, w is the width or lesser horizontal dimension of a building, or a structural member and l is the length or greater horizontal dimension of a building specified in IS: 875 (Part 3)-1987.

4 DOMAIN MESHING AND MODEL DETAILS

The arrangement used for the study of interference effects in high-rise building in CFD used two rectangular plan shape building having same dimension in same axis and parallel to each other placed inside the single domain. The regions of fluid flow and/or heat transfer in CFX are called domains. Fluid domains define a region of fluid flow, while solid domains are regions occupied by conducting solids in which volumetric sources of energy can be specified. Two buildings namely Building 1 is interfering building and Building 2 is principal building having Depth (D) = 250 mm, Width (W) = 100 mm, Height (H) = 500 mm and initial Spacing (S) =200 mm. The study based on two different wind angle like 0° and 90° in Figure 1. The domain used in this experiment as recommended by Frank et al. (2004) is the inlet, the lateral and the top boundary should be 5H away from the building and the outflow boundary should be placed at least 15H behind the building to allow for proper flow development shown in Figure 2. Where H is the building height. The space in lateral direction must larger than the building height.

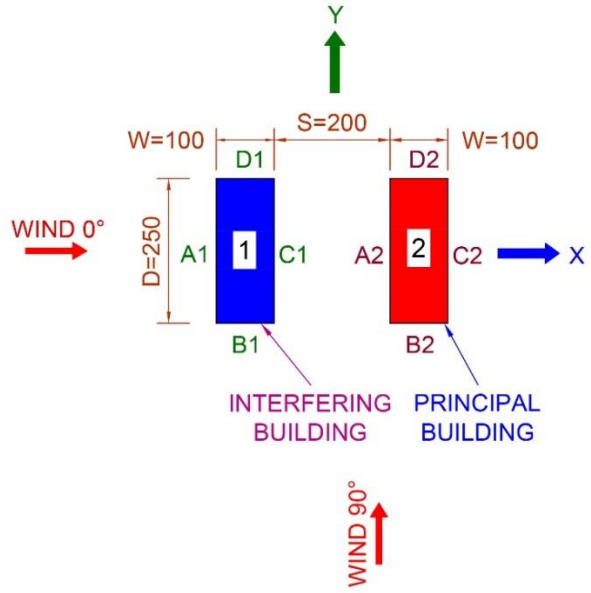

(a)

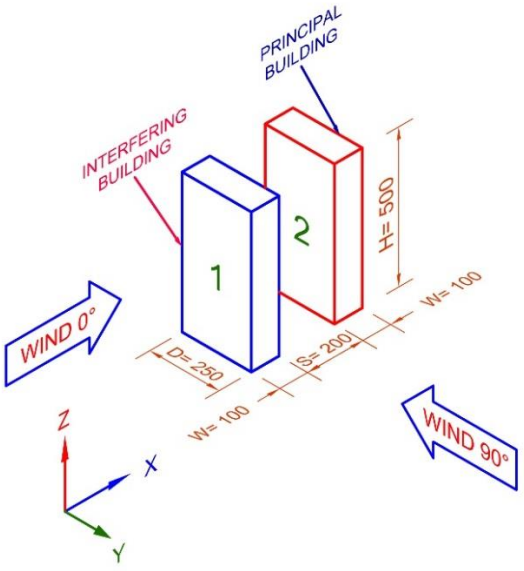

(b)

Figure 1. Details dimension and attacking wind angle of interfering and principal building (a) Plan view (b) Isometric view.

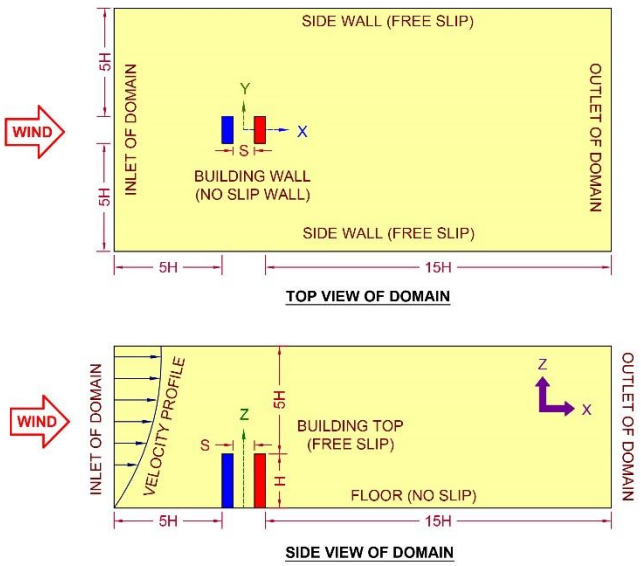

Figure 2. Detail dimension of domain.

The faces of interfering building are A1, B1, C1, D1 and principal building are A2, B2, C2, D2. The initial spacing between two buildings are 200 mm for both 0° and 90° wind angle. The spacing gradually increased at an interval of 1,000 mm up to 14,000 mm for 0° wind angle and at an interval of 100 mm up to 1,000 mm for 90° wind angle to reach its optimum spacing where the interference effect by the interfering building will nullify and the principal building will behave like isolated building. Mesh adaption in CFX is the process in which, once or more during a run, the mesh is selectively refined in areas that depend on the adaption criteria specified. This means that as the solution is calculated, the mesh can automatically be refined in locations where solution variables are hanging most rapidly, in order to resolve the features of the flow in these regions. The tetrahedron meshing used and inflated near the boundary to avoid the unusual flows. The detail of meshing are shown in Figure 3.

5 BOUNDARY CONDITION

The magnitude of the inlet velocity, the direction is taken to be normal to the boundary. The experimental flow was simulated similar to that of terrain category 2 as per Indian standard for wind load IS: 875 (part 3) - 1987 at a geometric scale of 1:300. The direction constraint requires that the flow direction is parallel to the boundary surface normal which is calculated at each element face on the inlet boundary. For no slip wall (not moving, no wall velocity) the velocity of the fluid at the wall boundary is set to zero, so the boundary condition for the velocity becomes: $U_{wall}=0$. For free slip wall the velocity component parallel to the wall has a finite value, but the velocity normal to the wall, and the wall shear stress, are both set to zero: $U_{wall}=0$, $\tau_w=0$. The velocity profile of the atmospheric boundary layer in the CFD are calculated by the following power law:

$$\frac{U}{U_H} = \left(\frac{Z}{Z_H}\right)^{\alpha} \tag{11}$$

where U is the horizontal wind speed at an elevation Z; U_H is the speed at the reference elevation Z_H; which was 10 m/s; α is the parameter that varies with ground roughness which is 0.133 for terrain category 2 and Z_H is 1.0 m for this case.

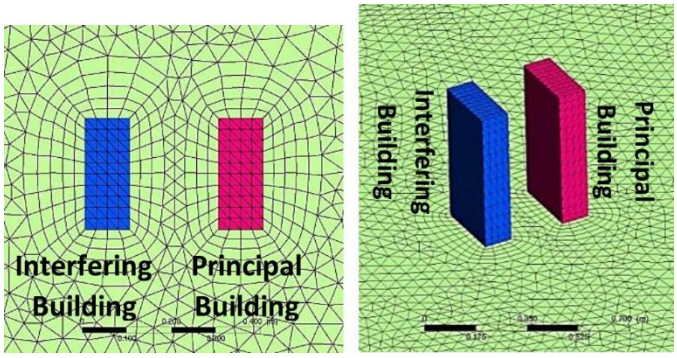

Figure 3. Meshing details of interfering and principal building.

The kinetic energy of turbulence and its dissipation rate at the inlet section are calculated according to the following equations:

$$k = \frac{3}{2}\left(U_{avg} I\right)^2 \text{ and } \varepsilon = C_{\mu}^{\frac{3}{4}}\left(\frac{k^{\frac{3}{2}}}{l}\right) \tag{12}$$

where U_{avg} is the mean velocity at inlet; I is the turbulence intensity; l is the turbulence integral length scale. The velocity profile of isolated building at 0° wind angle are shown in Figure 4.

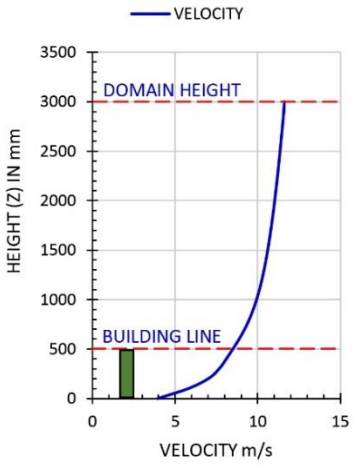

Figure 4. Velocity profile of isolated building for 0° wind angle.

6 EXPERIMENTAL AND ANALYTICAL RESULTS

Expected results of this study by CFX is quite similar with Wind tunnel test. Turbulence intensity for Interfering and Principal building is also calculated here shown in Figure 5. Comparing the velocity profile by CFX with previous experimental study by wind tunnel test from M. Tech thesis is given in Figure 6. The experimental data were obtained at the middle portion of interfering and principal building. Whereas in CFD a vertical line drawn at that location. Therefore velocity profile at that point for both experimental and analytical case are near about same.

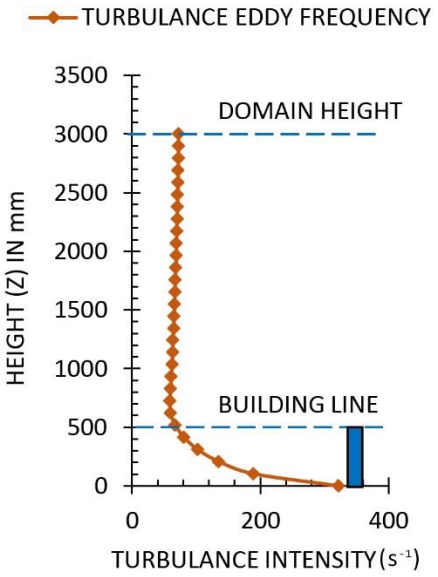

Figure 5. Longitudinal turbulence intensity for interfering and principal building.

7 RESULTS AND DISCUSSIONS

7.1. Average pressure coefficient

To reduce interference effect, the optimum spacing between interfering and principal building is suitable when pressure coefficient of all the faces of principal building shows same results of an isolated building as well as the interfering building. In this study the initial spacing between interfering and principal building is 200 mm. This spacing gradually increasing with 1,000 mm interval to reach optimum spacing. When wind angle is 0° the optimum spacing shows 14,000 mm (i.e. 56 times of upstream windward face of interfering building) and for 90° wind angle it is 1,000 mm (i.e. 10 times of upstream windward face of interfering building) in Figure 7 and Figure 8 respectively. As a guideline referred by Mendis et al. (2007) interference due to buildings of similar size to the subject building, located within a distance equal to 10 times the building width, need be considered. Which was satisfied by this studies. Figure 7 shows graphical representation of pressure coefficients of different faces at various spacing between interfering and principal building. The C_{pe} of different faces of isolated building are highlighted by dotted line. In this figure the C_{pe} is negative value i.e. suction for face A2 at initial spacing 200 mm, and the pressure goes to positive direction by increasing the spacing. When the spacing reaches 900 mm the C_{pe} shows positive in nature. For spacing 7,000 mm C_{pe} of face A2 and C2 are close to average pressure coefficient of isolated building. In this case other related face, the pressure for face B2 and D2 are not closer to the respective faces of isolated building. Therefore this spacing may not be optimum. After some iteration spacing reaches 14,000 mm and the C_{pe} values are shown to their same respective face pressure as isolated building. Here the C_{pe} values of face B2 and D2 are same for all spacing variations.

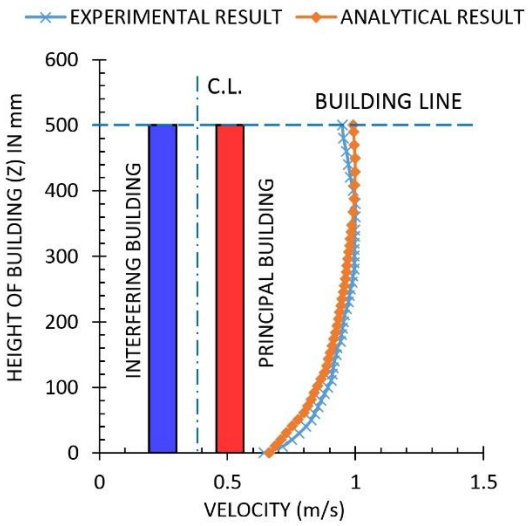

Figure 6. Comparison between experimental and analytical data of velocity profile in between interfering and principal building at 90° wind angle.

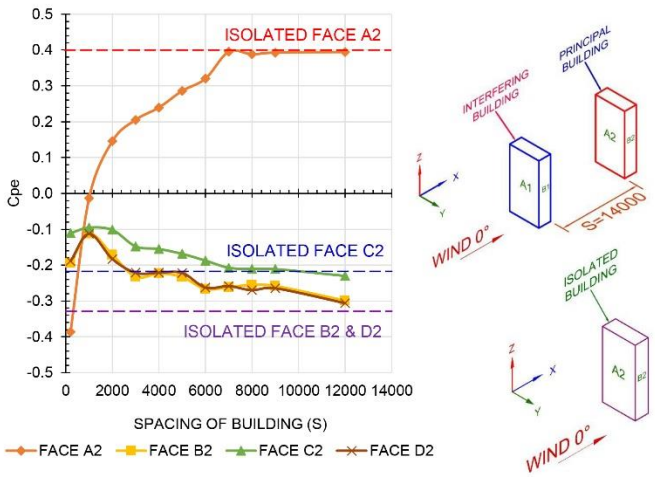

Figure 7. Cpe for optimum spacing 14,000 mm at 0° wind angle.

Figure 8 shows positive face pressure for B2 only which facing upstream wind flow for 90° wind angle. This case initial spacing between interfering and principal building is 200 mm and increment of spacing is 100 mm. The optimum spacing lies 1,000 mm where C_{pe} are same for all the respective face as isolated building. An interesting parameter noted here, the face A2 and C2 are not showing same values except the optimum spacing 1,000 mm. From initial spacing to 600 mm spacing the difference of C_{pe} is higher for both the face A2 and C2. This values are comes closer towards the optimum spacing. The C_{pe} of spacing between 200 mm to less than 1,000 mm are different due to unsymmetrical reattachment of interfering and principal building.

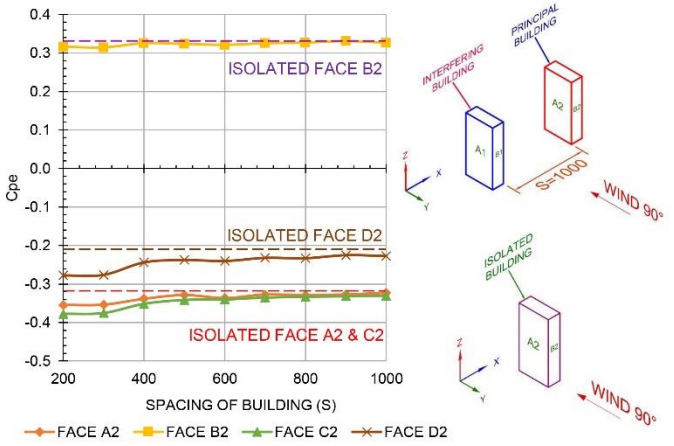

Figure 8. Cpe for optimum spacing 1,000 mm at 90° wind angle

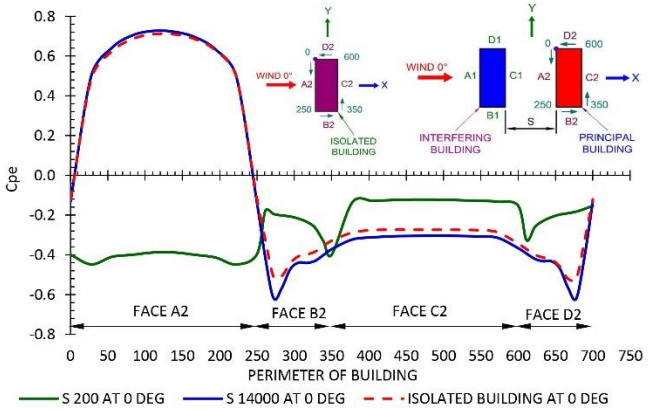

Figure 9. Comparison of horizontal Cpe for different faces of isolated and principal building at height H/2 at 0° wind angle.

The comparative study between isolated building, initial spacing at 200 mm and optimum spacing 14,000 mm for interfering and principal building are shown by graphical representation in Figure 9 and 10. The horizontal face pressure at H/2 of isolated building and principal building for spacing 200 mm and 14,000 mm for 0° and 90° wind angle are accepted. From both the figure it is clear that when optimum spacing lies 14,000 mm for 0° wind angle and 1,000 mm for 90° wind angle the values of C_{pe} of all the faces of principal building are supports the C_{pe} of all the faces of isolated building. At initial spacing 200 mm C_{pe} values of isolated and principal building are drastically different.

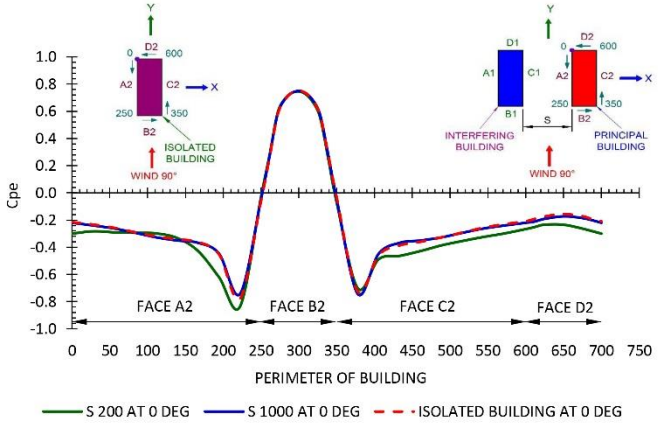

Figure 10. Comparison of horizontal Cpe for different faces of isolated and principal building at height H/2 at 90° wind angle.

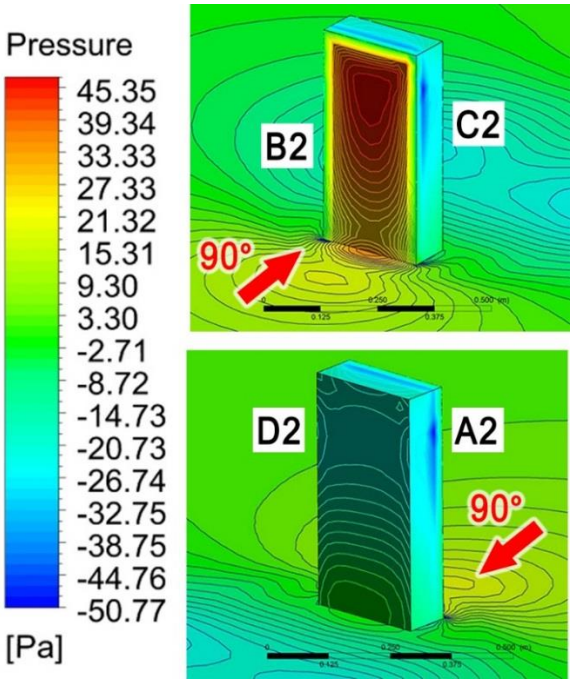

Figure 11. Front and back side view of pressure contour of different faces for isolated building at 0° wind angle.

The isometric view of pressure contour of different faces of isolated building and at optimum spacing of interfering and principal building are shown in Figure. 11-14. The comparative statement of pressure couture and stream line for isolated building and initial spacing 200 mm and optimum spacing 14,000 mm for 0° wind angle and initial spacing 200 mm and optimum spacing 1,000 mm for 90° wind

angle for interfering building and principal building are shown in Table 2 and 3.

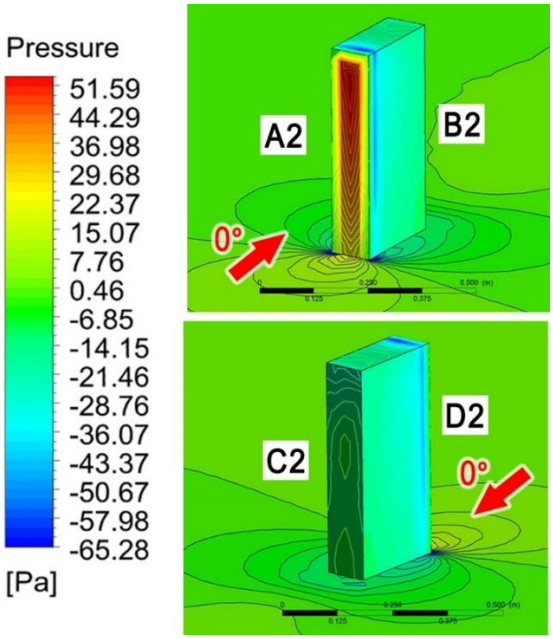

Figure 12. Front and back side view of pressure contour of different faces for isolated building at 90° wind angle.

8 INTERFERENCE FACTOR (IF)

The interference effect due to wind an Interference Factor (IF) has been introduces as a multiplying factor to be applied to the design wind pressure/force. IF can be more significant for tall buildings. The value of IF varies according to the building geometry, location, spacing between the buildings. The given values of IF are a kind of median values and are meant only for preliminary design estimates. IF is usual to express the effect of interference in terms of the ratio of the modified pressure/force due to interference and the wind pressure/force without any interference (i.e., stand-alone condition). This non-dimensional term is called Interference Factor (IF). Numerically Interference Factor (IF) expressed in below.

$$Interference\ Factor\ (IF) = \frac{Mean\ wind\ pressure\ (or\ wind\ force\ or\ dynamic\ responce)\ of\ the\ Pincipal\ building\ under\ interference}{Mean\ wind\ pressure\ (or\ wind\ force\ or\ dynamic\ responce)\ of\ the\ Isolated\ building}$$

This study also highlight the Interference Factor (IF) which is gradually changes from negative to positive direction for 0° wind angle at face A2 and B2 for initial spacing. For 0° wind angle and 90° wind angle the optimum spacing between interfering and principal buildings are 14,000 mm and 1,000 mm respectively. Which is 56 times and 10 times of upstream windward face of interfering building for the aspect ratio 5:2.5:1 (H:D:W). In Figure 15 (a) and (b) shows a typical condition of upstream wind angle in X and Y axis of same dimension and aspect ratio consideration of interfering and principal building. Considering the depth of upstream windward face of interfering building is X and spacing between interfering and principal building is S. By this consideration the interference factors of different faces of principal building are plotted in graphical representation as shown in Figure 16 (a) and (b) .

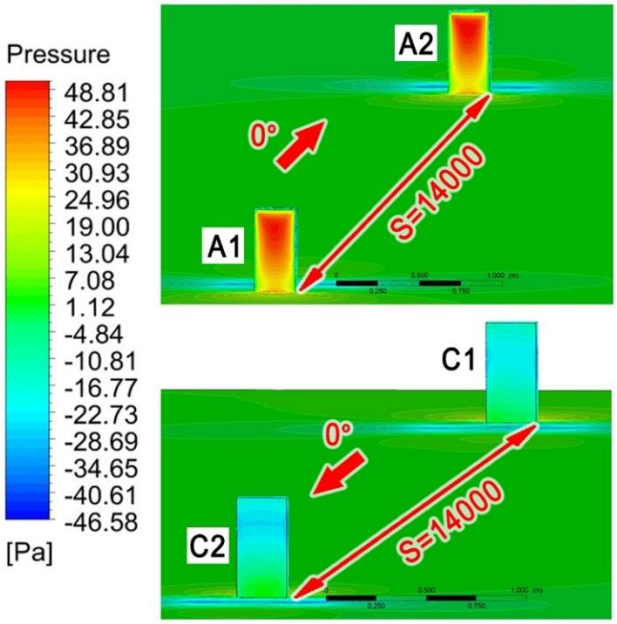

Figure 13. Front and back side view of pressure contour of different faces for interfering and principal building at optimum spacing (S=14,000 mm) at 0° wind angle.

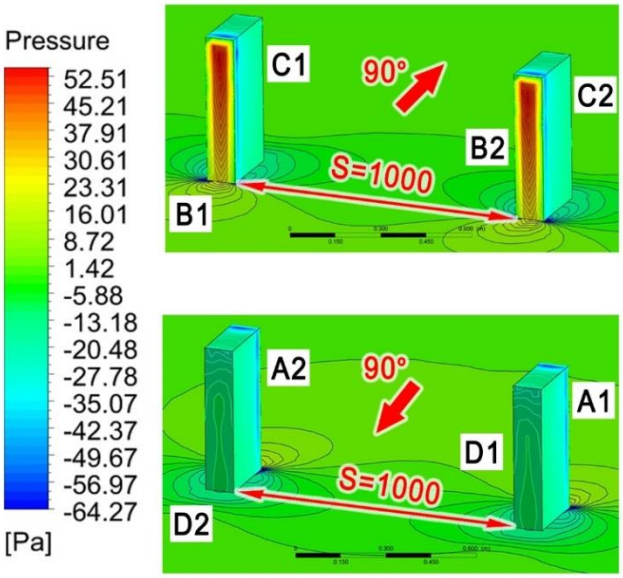

Figure 14. Front and back side view of pressure contour of different faces for interfering and principal building at optimum spacing (S=1,000 mm) at 90° wind angle.

Table 2: Comparative statement for pressure contour and stream line of different faces of isolated building, interfering building and principal building at 0° wind angle.

Building face	Isolated building	Spacing (S) 200 mm		Spacing (S) 14,000 mm	
		Interfering building (Building: 1)	Principal building (Building: 2)	Interfering building (Building: 1)	Principal building (Building: 2)
	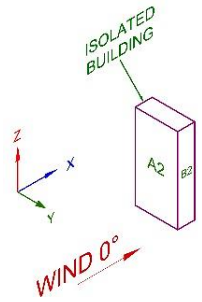	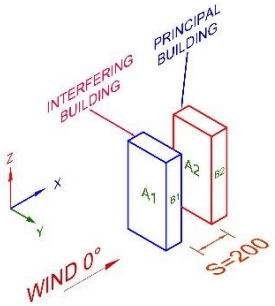		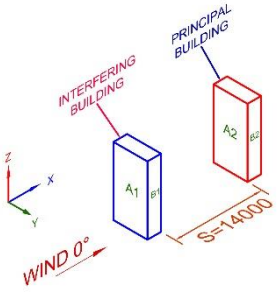	
	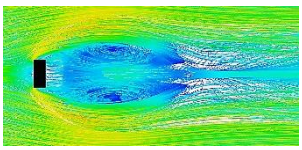	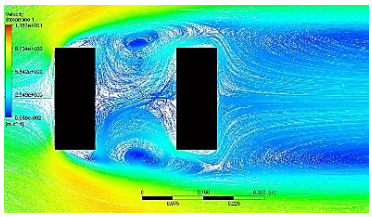		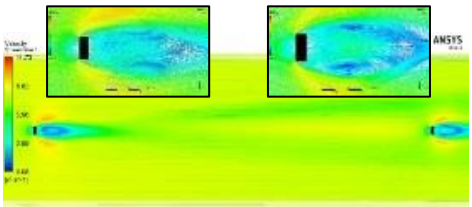	
Face A	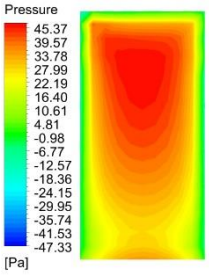	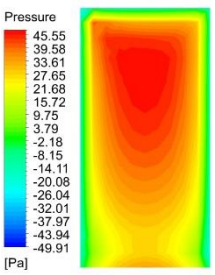	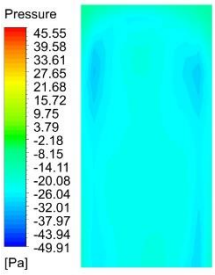	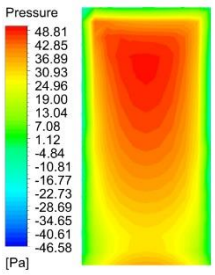	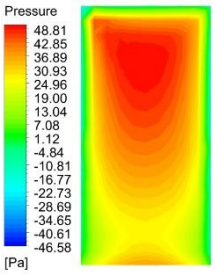
Face B	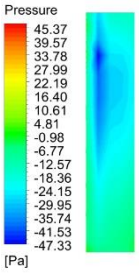	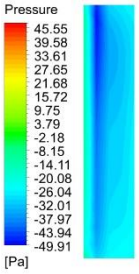	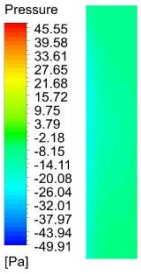	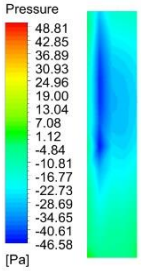	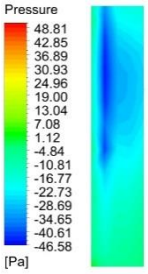
Face C	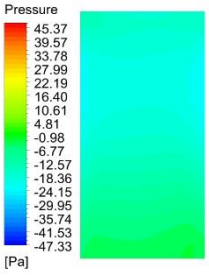	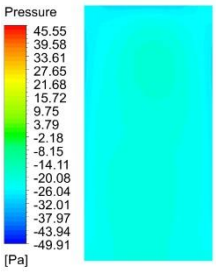	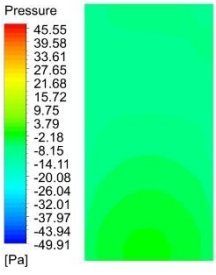	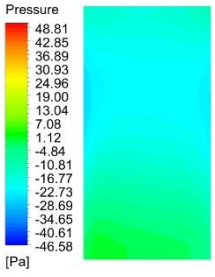	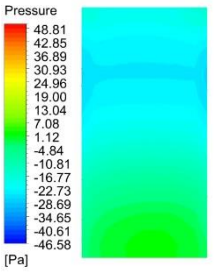
Face D	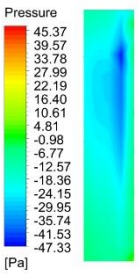	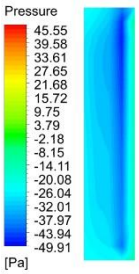	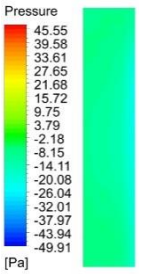	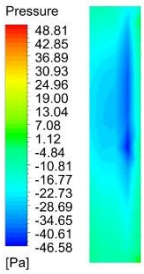	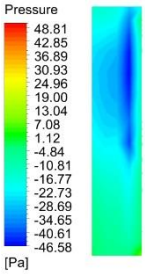

Table 3: Comparative statement for pressure contour and stream line of different faces of isolated building, interfering building and principal building at 90° wind angle.

Building face	Isolated building	Spacing (S) 200 mm		Spacing (S) 1,000 mm	
		Interfering building (Building: 1)	Principal building (Building: 2)	Interfering building (Building: 1)	Principal building (Building: 2)
	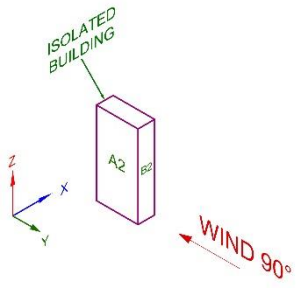	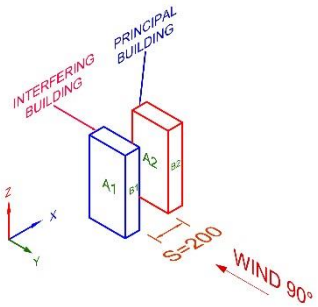		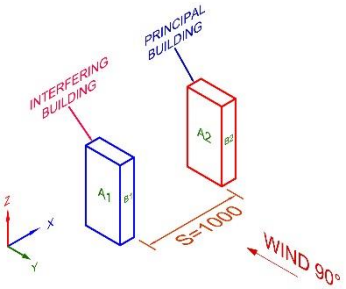	
		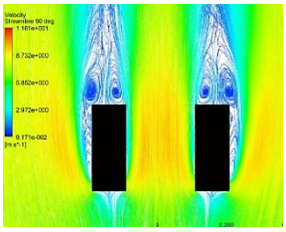		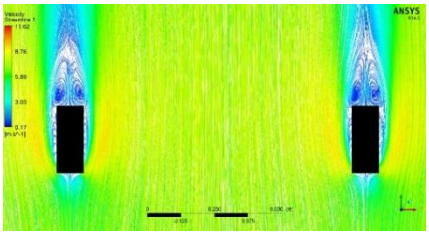	
Face A	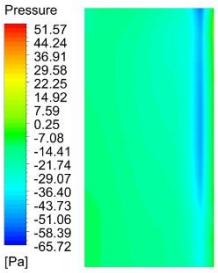	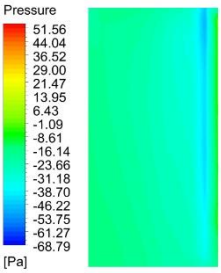	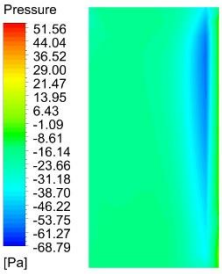	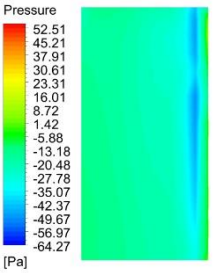	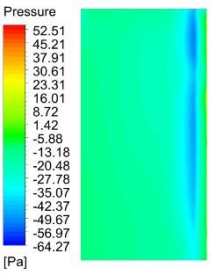
Face B	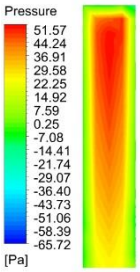	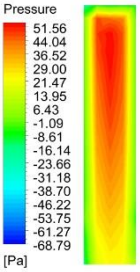	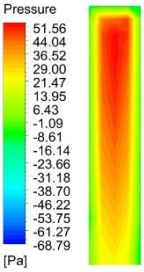	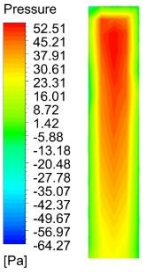	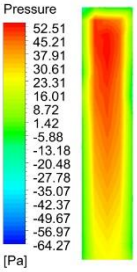
Face C	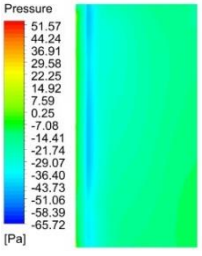	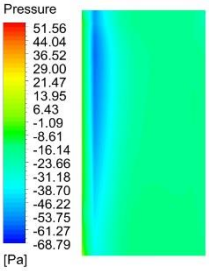	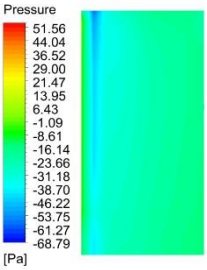	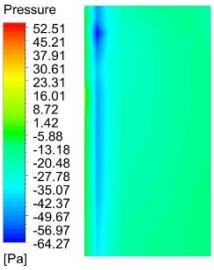	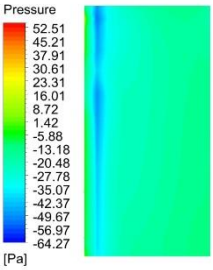
Face D	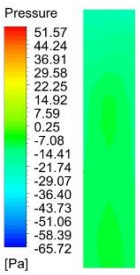	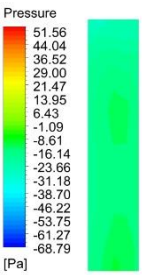	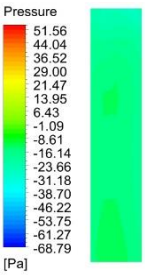	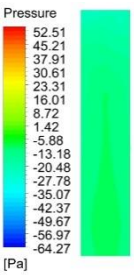	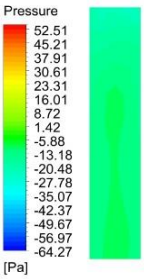

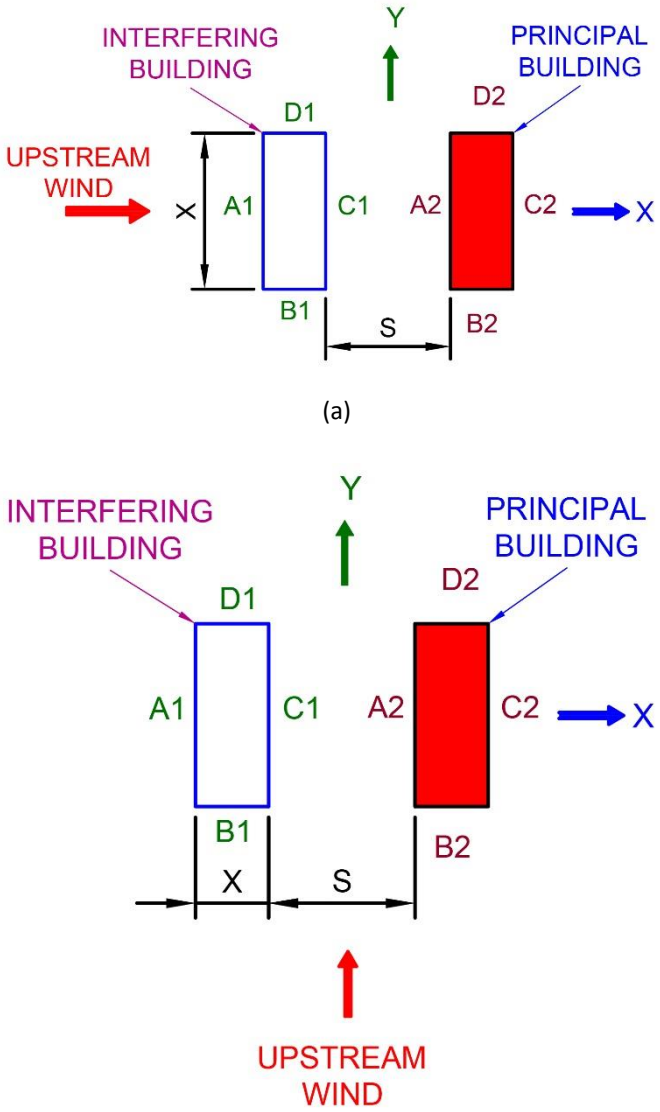

Figure 15. Typical condition of upstream wind angle of same dimension and aspect ratio of interfering and principal building (a) Upstream wind in X direction (b) Upstream wind in Y direction.

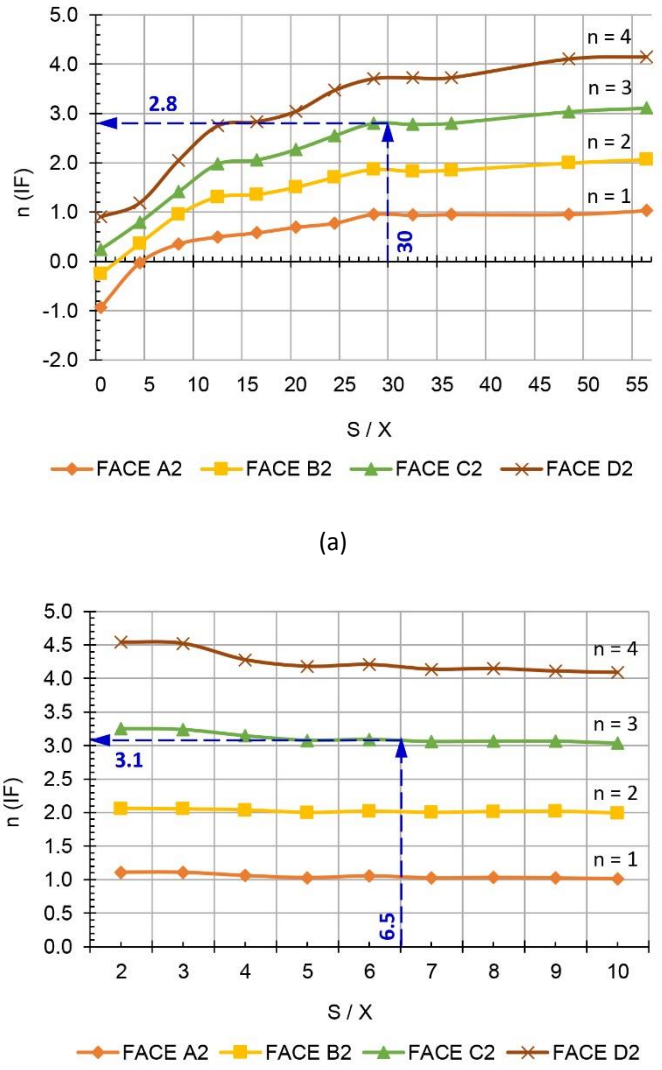

Figure 16. Graphical representation to calculate IF for different spacing between interfering and principal building due to upstream wind angle of same dimension and aspect ratio of the buildings (a) Upstream wind in X direction (b) Upstream wind in Y direction.

From the graphical representation shown in Figure 16 (a) and (b), all the faces are denoted as *n=1, 2, 3* and *4* starting from face A2. Horizontal axis in graph denotes the ratio of spacing *(S)* to the depth of upstream windward face of interfering building *(X)*. The vertical axis denotes *n(IF)*. From Figure 14 (a) considering a *(S/X)* ratio *30* and plot it to *n=3* graph i.e. for face C2 and collect the respective value of n(*IF)* from graph, it's *2.8*. By this value IF are calculated by dividing *n* values i.e. *n=3*. Therefore, the calculated IF for face C2 of principal building be *0.93*. This procedure repeated for upstream wind in Y axis also. From the Figure 14 (b) *(S/X)=6.5* and respective *n(IF)=3.1* for *n=3*. Therefore IF be *1.03* for face C2 of principal building.

9 CONCLUSION

The present study based on number of CFD simulations to determine optimum spacing between two high-rise buildings like interfering and principal building where interference effects will nullify or the principal building behave like an isolated building. During this study it is found that the optimum spacing between interfering and principal building for wind angle 0° and 90° are 14,000 mm and 1,000 mm respectively. Which is 56 times and 10 times of upstream windward face of interfering building in X and Y axis respectively. At this optimum spacing the C_{pe} values of principal building are same as isolated building. The spacing between interfering and principal buildings are gradually increasing to obtain IF 1.0. After reaching optimum spacing at 0° and 90° wind angle, IF shows 1.0 i.e. behavior of principal building is same as the isolated building. During the

study different wind angles and different spacing's are also tested in CFD simulation. A typical relation are found between windward face of interfering building and spacing between interfering and principal building by which IF can be calculated for different face of principal building at upstream wind angle along X and Y axis. After the rigorous analysis, the above information are quite helpful for structural designer to estimate the proper wind load for such type of terrain, geometrical configurations and interference conditions.

10 REFERENCES

Agerneh K. D., Girma T. B., Ryan M (2009), "Computational evaluation of wind pressures on tall buildings". *11th Americas Conference on Wind Engineering*, San Juan, Puerto Rico, June 22-26.

Ahuja, A.K., Dalui, S.K., Ahuja, R., Gupta, V.K. (2005), "Effect of interference on the wind environment around high-rise buildings", *Journal of Wind Engineering & Science*, Vol. 2, No. 1, July, pp. 1-8.2310.

"ANSYS CFX-Solver Theory Guide", Release 14.5, October 2012.

Bazdidi-Tehrani, F., Ghafouri, A., Jadidi, M, (2013), "Grid resolution assessment in large eddy simulation of dispersion around an isolated cubic building". *Journal of Wind Engineering and Industrial Aerodynamics*, 121, 1–15.

Blocken, B., Carmeliet, J., Stathopoulos, T. (2007), "CFD evaluation of wind speed conditions in passages between parallel buildings—effect of wall-function roughness modifications for the atmospheric boundary layer flow". *Journal of Wind Engineering and Industrial Aerodynamics*, 95, 941–962.

Braun, A.L., Awruch, A. M. (2009), "Aerodynamic and aeroelastic analyses on the CAARC standard tall building model using numerical simulation". *Computers and Structures*, 87, 564–581.

Dalui, S.K., (2005), "Experimental Investigation of parameters influencing wind environment around buildings", M. Tech Thesis, *Indian Institute of Technology, Roorkee, India.*

Franke, J., Hirsch, C., Jensen, A., Krüs, H., Schatzmann, M., Westbury, P., Miles, S., Wisse, J. and Wright, N.G. (2004), "Recommendations on the use of CFD in wind engineering, COST Action C14", *Impact of Wind and Storm on City Life and Built Environment, von Karman Institute for Fluid Dynamics.*

Gu. M. (2009), "Study on wind loads and responses of tall buildings and structures". *The seventh Asia-pacific conference on Wind engineering*, November 8-12, 2009, Taipei, Taiwan.

Gu, M., Xie, Z. N. (2011), "Interference effects of two and three super-tall buildings under wind action", *Acta Mech. Sin.*, 27(5): 687–696.

Hui. Y., Tamura Y., Yoshida A. (2012), "Mutual interference effects between two high-rise building models with different shapes on local peak pressure coefficients", *Journal of Wind Engineering and Industrial Aerodynamics*, 104–106, 98–108.

Hui, Y., Yoshida, A., Tamura, Y. (2013), "Interference effects between two rectangular-section high-rise buildings on local peak pressure coefficients". *Journal of Fluids and Structures* 37, 120–133.

I.S: 875 (Part-3) 1987, "Indian Standard Code of practice for the design loads (Other than Earthquake) for buildings and structures (Part-3, Wind Loads)", Bureau of Indian Standards, New Delhi, India.

Kim, W., Tamura, Y., Yoshida, A. (2009), "Interference effects of local peak pressures acting on walls of tall buildings". *11th Americas Conference on Wind Engineering*, San Juan, Puerto Rico, June 22-26.

Krishna, P., Kumar, K., Bhandari, N. M. "IS: 875(Part3): Wind Loads on Buildings and Structures -Proposed Draft & Commentary". Document No.: IITK-GSDMA-Wind 02-V5.0, IITK-GSDMA-Wind 04-V3.0, *Final Report: B - Wind Codes IITK-GSDMA Project on Building Codes.*

Luo, Z., Li, Y., Rosler, M., Seifert, J. (2008), "Surrounding buildings and wind pressure distribution on a high-rise building", *9th International Symposium on building and urban environmental engineering*, 7-10 July, Hong Kong.

P. Mendis, T. Ngo, N. Haritos, A. Hira, B. Samali, J. Cheung (2007) "Wind Loading on Tall Buildings". *EJSE Special Issue: Loading on Structures.*

Peng, X., Zhang, C. and Qiao, C. (2009), "Numerical simulation of static interference effects for single buildings group". *The seventh Asia-pacific conference on Wind engineering*, November 8-12, Taipei, Taiwan.

Tehrani, F. B., Ghafouri, A., Jadidi, M. (2013), "Grid resolution assessment in large eddy simulation of dispersion around an isolated cubic building", *Journal of Wind Engineering and Industrial Aerodynamics*, 121, 1–15.

Tominaga, Y., Stathopoulos, T. (2013), "CFD simulation of near-field pollutant dispersion in the urban environment: A review of current modelling techniques". Atmospheric Environment, 79, 716-730.

Xie, Z.N., Gu, M. (2004), "Mean interference effects among tall buildings". *Engineering Structures*, 26, 1173–1183.

Yoon, D.H., Yang, K.S, Choi, C.B. (2011), "Three-dimensional wake structures and aerodynamic coefficients for flow past an inclined square cylinder", *Journal of Wind Engineering and Industrial Aerodynamics*, 101, 34–42.

Zhang, A., Zhang, L. (2004), "RBF neural networks for the prediction of building interference effects". *Computers and Structures*, 82, 2333–2339.

Zhang, A., Gu, M. (2008), "Wind tunnel tests and numerical simulations of wind pressures on buildings in staggered arrangement". *Journal of Wind Engineering and Industrial Aerodynamics*, 96, 2067–2079.